

NASA CONTRACTOR REPORT 177396

AN ANALYSIS OF SOUND ABSORBING LININGS FOR THE INTERIOR
OF THE NASA AMES 80X120-FOOT WIND TUNNEL

(NASA-CR-177396) AN ANALYSIS OF SOUND
ABSORBING LININGS FOR THE INTERIOR OF THE
NASA AMES 80 X 120-FOOT WIND TUNNEL (Astron
Research and Engineering) 47 p C SCL 20A

N88-13006

g3/71 Unclass
0111220

J.F. Wilby
P.H. White
Astron Research and Engineering
3228 Nebraska Avenue
Santa Monica, CA 90404

CONTRACT NAS2-A-32501-C

NASA

National Aeronautics and
Space Administration

Ames Research Center
Moffett Field, California 94035

TABLE OF CONTENTS

	<u>Page</u>
LIST OF FIGURES	ii
1.0 INTRODUCTION	1
2.0 ANALYTICAL MODEL	3
3.0 VALIDATION EXPERIMENT	8
3.1 Test Requirements	8
3.2 Test Site	8
3.3 Test Description	9
3.4 Test Results	11
4.0 LINING ANALYSIS	14
4.1 Lining Materials and Configurations	14
4.2 Parametric Study	16
4.3 Protection from Erosion	20
5.0 CONCLUSIONS	21
REFERENCES	23
FIGURES	24

LIST OF FIGURES

<u>Figure</u>		<u>Page</u>
1	Section through Multi-Element Lining	24
2	Section through Typical Wall Treatment for B-1B Ground Run-Up Noise Suppressor	25
3	Sketch of Test Set-Up	26
4	Microphone Calibration Spectra	27
5	Sample Test Data (Microphone Separation Distance = 1.5 in)	28
6	Comparison of Measured and Predicted Sound Absorption Coefficients for B-1B Run-Up Noise Suppressor	29
7	Comparison of Predicted and Band-Averaged Measured Sound Absorption Coefficients for B-1B Ground Run-Up Noise Suppressor	30
8	Effect of Angle of Incidence on Predicted Sound Absorption Coefficient (Lining Configuration 1)	31
9	Lining Configurations Considered in Analysis	32
10	Predicted Sound Absorption Coefficients for Owens Corning PF 3350 and 703 Fiberglass (Configuration 1)	33
11	Predicted Sound Absorption Coefficients for Owens Corning PF 3350 and 701 Fiberglass (Configuration 1)	34
12	Effect of Thickness of PF 3350 Fiberglass on Predicted Sound Absorption Coefficient (Lining Configuration 1)	35
13	Effect of Air Gap on Predicted Sound Absorption Coefficient (Lining Configurations 1 and 2)	36
14	Effect of Fiberglass Cloth Flow Resistance on Predicted Sound Absorption Coefficient (Lining Configuration 2)	37

<u>Figure</u>		<u>Page</u>
15	Effect of Perforated Backing Plate on Predicted Sound Absorption Coefficient (Lining Configuration 3)	38
16	Effect of Thickness of Perforated Plate on Predicted Sound Absorption Coefficients (Configuration 1)	39
17	Effect of Perforated Plate Open Area on Predicted Sound Absorption Coefficients (Configuration 1) . .	40
18	Protective Facings for Acoustical Linings Subjected to High Velocity Gas Flows (Reference 4)	41

1.0 INTRODUCTION

In order to make full use of the NASA Ames 80x120-foot wind tunnel, it is necessary that the interior surfaces of the tunnel be covered with sound-absorbing material. NASA has performed an initial design of the acoustic treatment but desired that additional studies be performed to evaluate the sound absorption characteristics of candidate treatments in both the low and mid-frequency regimes. The low frequency range is of interest with regard to use of the test section for helicopter noise measurements and the mid-frequency range is a critical factor for noise in the surrounding community.

The interest in absorption coefficients at frequencies below 125 Hz poses certain problems with regard to the testing of treatments. Conventional test procedures involve the placement of sample materials in a reverberant chamber and the measurement of the reverberation times of the chamber with and without the material present. For example, the ASTM standard procedure [1] requires that the smallest dimension of the test chamber should be more than one wavelength, and preferably more than two wavelengths of the center frequency of the lowest one-third octave band at which measurements are made. This would require a chamber with a minimum dimension of 22 to 44 feet if measurements were to be made at 50 Hz. Very few chambers of this size are available. However, the recent construction of a ground run-up suppressor for the Rockwell International B-1B airplane provided an opportunity for acoustic measurements since the walls of the enclosure were covered with sound absorbing material designed for high sound absorption at low frequencies.

In the present study an analytical model is constructed to predict the sound absorption coefficients of multi-element sound absorbing treatments. The model is validated by comparison with test data

from B-1B noise suppressor tests and it is then used to evaluate different treatment designs for the interior of the 80x120 ft wind tunnel. Section 2 of this report presents an outline of the analytical model, Section 3 describes the acoustic tests in the B-1B noise suppressor and Section 4 discusses various lining configurations. The findings of the study are summarized in Section 5.

2.0 ANALYTICAL MODEL

An early study of sound-absorbing linings for the 80x120 ft wind tunnel was conducted by Rennison, Wilby and Gordon [2] in 1978. That study considered several materials but the treatments were limited to four-element systems containing a porous face plate, a bulk material and an air gap backed by a rigid surface. The analytical approach used in that study forms the basis for the present work, but the analysis is extended to include a greater variety of elements in the lining, and a greater range in acoustic properties of the bulk material.

The type of treatment being considered is shown in Figure 1. It consists of a perforated plate which protects the material from erosion by the flow in the tunnel, a porous layer which could be a combination of a wire mesh screen and fiberglass cloth, a bulk material such as a fibreglass blanket, a second porous layer which again could consist of fiberglass cloth with or without a perforated plate, a second bulk material or an air gap, and finally a rigid wall.

In the analysis of multi-layer systems such as the one shown in Figure 1, Zwicker and Kosten [3] and Beranek [4] have shown that the propagation and attenuation of sound in one of the layers may be described by the following parameters:

$k_n = \alpha'_n + i\beta_n$, the propagation constant for the nth layer,

α'_n = the attenuation constant for the nth layer,

β_n = the phase constant for the nth layer,

$W_n = -(iKk_n) / (\omega Y)$, the complex characteristic or wave impedance for the nth layer,

Y = the porosity of the layer,

K = the complex compressibility of the layer.

The impedance of a finite thickness (nth) layer may be written in the form [3]

$$z_n = W_n \frac{z_{n+1} \cosh k_n L_n + W_n \sinh k_n L_n}{z_{n+1} \sinh k_n L_n + W_n \cosh k_n L_n} \quad (1)$$

where z_{n+1} is the impedance of the backing medium, and W_n and k_n are, respectively, the wave impedance and the propagation constant in the nth layer.

For layer $n = 4$ in Figure 1, $z_{n+1} = z_5 = \infty$ for a rigid wall. Furthermore, if the 4th layer is an air gap, $W_n = W_4 = \rho c$, and $k_n = k_4 = ik = i\omega/c$, then

$$z_4 = \rho c \coth(k_4 L_4) = -i\rho c \cot(kL_4). \quad (2)$$

From Ingard and Bolt [5], the propagation constant k_3 for the porous layer (3rd layer) of thickness L_3 can be given by:

$$k_3 = \left[\left(S_3 + \frac{iR_3}{\omega\rho L_3} \right) P_3 \gamma_0 \right]^{1/2} \frac{\omega}{c} \quad (3)$$

where R_3 = flow resistance of material of thickness L_3

S_3 = material structure factor

P_3 = porosity of material

γ_0 $\begin{cases} = 1.4 \text{ for isothermal conditions (low frequencies)} \\ = 1.0 \text{ for adiabatic conditions.} \end{cases}$

The characteristic impedance of the layer is given by:

$$W_3 = \rho c \left[\left(S_3 + \frac{iR_3}{\omega \rho L_3} \right) \frac{1}{P \gamma_0} \right]^{1/2} \quad (4)$$

Using Eq. (1),

$$\frac{Z_3}{\rho c} = \frac{1 + (\rho c/Z_4)(W_3/\rho c) \tanh(k_3 L_3)}{(\rho c/W_3) \tanh(k_3 L_3) + (\rho c/Z_4)} \quad (5)$$

Characteristics of the fiberglass layer can be estimated using relationships given by Beranek [4]. From Table 10.4 of [4], the propagation constant k_2 , where

$$k_2 = \alpha_2' + i \beta_2,$$

can be estimated from empirical expressions for the real and imaginary parts (with $f = \omega/2\pi$):

$$\alpha_2' = (\omega/c) [0.189 (\rho f/R_2)^{-0.595}] \quad (6)$$

and

$$\beta_2 = (\omega/c) [1 + 0.0978 (\rho f/R_2)^{-0.70}] \quad (7)$$

The characteristic impedance W_2 is then given by (Eq 10.18, [4])

$$W_2 = (-iKk_2)/(\omega Y) \quad (8)$$

K , the compressibility of air in the porous medium, is obtained from Figure 10.6 of [4]. Then, the impedance Z_2 is evaluated by means of Eq.(1)

In the case of the outer perforated plate and porous layer, use is made of the results of Guess [6] and the associated discussion in [2]. The impedance of the perforated plate and porous layer combined can be written as:

$$\frac{Z'}{\rho c} = \left\{ \frac{R_1}{\sigma \rho c} + \frac{\sqrt{8\nu\omega}}{\sigma c} (1+t/d) + \frac{(kd)^2}{8\sigma} \right\} + i \left\{ \frac{\omega(t+\delta)}{\sigma c} + \frac{\sqrt{8\nu\omega}}{\sigma c} (1+t/d) + \frac{\omega S_1 L_1}{\sigma c} \right\} \quad (9)$$

where

- R_1 = flow resistance of material of thickness L
- S_1 = material structure factor
- σ = fractional open area of perforated plate
- t = thickness of perforated plate
- d = hole diameter in perforated plate
- L_1 = thickness of porous layer
- δ = $0.85d$ for zero Mach number in the external flow
- ν = kinematic viscosity of acoustic medium.

Then, the impedance of the perforated plate and porous layer can be added to that of the backing layers, so that:

$$Z_1 = Z_2 + Z' \quad (10)$$

The absorption coefficient for normal incidence can now be obtained from

$$\alpha(0^\circ) = 1 - |(Z_1 - \rho c)/(Z_1 + \rho c)|^2 \quad (11)$$

Following Morse and Ingard [7], the value of the absorption coefficient for a given angle of incidence ψ is given by

$$\alpha(\psi) = 1 - \left| (Z_1 \cos \psi - \rho c) / (Z_1 \cos \psi + \rho c) \right|^2 \quad (12)$$

and the average (statistical) value of the absorption coefficient is given by

$$\alpha_s = \frac{8\theta}{\theta^2 + \chi^2} \left[1 - \frac{\theta}{\theta^2 + \chi^2} \log_e (\theta^2 + \chi^2 + 2\theta + 1) + \frac{1}{\chi} \left(\frac{\theta^2 - \chi^2}{\theta^2 + \chi^2} \right) \tan^{-1} \left(\frac{\chi}{1 + \theta} \right) \right] \quad (13)$$

where $Z/\rho c = \theta - i\chi$.

3.0 VALIDATION EXPERIMENT

3.1 Test Requirements

The requirement of the validation experiment was to provide sound absorption data at low frequencies under conditions such that the data were not affected significantly by the test environment. Acoustic reverberant chambers normally used for sound absorption tests satisfy test standards at frequencies down to about 125 Hz, but the rooms are too small for satisfactory tests at lower frequencies. Furthermore, the test panels have to be large in order that edge diffraction effects do not dominate the data. The B-1B ground run-up noise suppressor satisfies both requirements in that it is a large enclosure and the sound-absorbing panels cover a large wall area.

3.2 Test Site

The tests were conducted in the B-1B ground run-up noise suppressor at Site 3, Plant 42, of the Rockwell International manufacturing facility at Palmdale, CA. The suppressor is constructed from an acoustic design developed by the authors of this report. The open-top pen design is intended to provide a moderate degree of noise reduction for local plant personnel and for the neighboring community. Additionally, the suppressor interior acoustic treatment has been designed with the goal that it not cause reflections which would increase the sound pressure levels on the surface of the aircraft above those encountered in an open stand or free field run-up. Thus the lining is required to have high acoustic absorption, and the suppressor provides a good opportunity to evaluate an analytical model for predicting the low frequency absorption of a treatment.

The lining used in the suppressor consists of an 8-inch thick

layer of PF 3530 glass fiber material (0.84 lb/cu.ft.) backed by a 2-inch air space. The glass fiber wool is covered by glass fiber cloth, stainless steel mesh, and a perforated steel cover with a 33% open area. A typical construction detail is shown in Figure 2.

3.3. Test Description

Determination of the normal incidence acoustic absorption properties of the lining is based on measurement of the acoustic impedance of the panels as installed in the suppressor. By exciting the test wall with a normally incident sound wave generated far away, and measuring the pressure at two points near the wall it is possible to estimate the local pressure and normal velocity. The surface impedance may then be calculated from these quantities [8].

The measured impedance Z_m can be expressed in terms of the transfer function $H_{12}(\omega)$ between the microphones.

$$Z_m = i\omega\rho d_{12} [1 + H_{12}(\omega)] / 2[1 - H_{12}(\omega)] \quad (14)$$

The normalized surface impedance is estimated by

$$Z/\rho c = [Z_m - i\rho c \tan(\omega d/c)] / [\rho c - iZ_m \tan(\omega d/c)] \quad (15)$$

and the normal absorption coefficient by

$$\alpha(0^\circ) = 1 - \left| [Z/\rho c - 1] / [Z/\rho c + 1] \right|^2 \quad (16)$$

The test set-up is shown in Figure 3. Two 1/2 inch diameter Bruel and Kjaer microphones were used. Microphone #1 was a B&K Type 4155 with an output of 1.191 volts for 124 dB SPL and microphone #2 was a B&K Type 4133 with an output of 3.33 volts at 124 dB. Both microphones were connected to GenRad Model 1560-P42 preamplifiers.

Acoustic excitation was provided by a random noise source driving two loudspeakers simultaneously. The distance between the loudspeakers and the microphones (58 feet) was large enough that curvature effects of the acoustic wave front were insignificant. Both the acoustic sources and microphones were at a height of approximately 20 inches above the concrete floor. Under these conditions a coherent, but out of phase, floor reflection occurs to cause destructive interference at a frequency of about 8000 Hz. By considering only the frequency range up to 500 Hz this floor effect is negligible.

Microphone signals were processed on a Hewlett-Packard Model 3582A Spectrum Analyzer. This analyzer computes the individual spectra of the microphone signals, as well as the cross spectrum, phase, and coherency. For this test, the controls were set to generate spectral components at 8 Hz increments from 0 to 1000 Hz (125 spectral lines). By taking 128 half-second samples and averaging the spectral components, a large value of the Bandwidth X Average Time product was obtained. The resulting data values have very small statistical variability. The output of the analyzer gives the transfer function to three significant figures and the phase angle to the nearest integer. This relatively low precision has an influence on the accuracy of the final estimates of the absorption coefficient.

Several simple calibration checks were performed. The transfer function derived from pistonphone calibration measurements was found to have a value of 2.796, due to the differences in microphone sensitivity. Spectral analysis of a test signal applied simultaneously to both channels of the analyzer shows a variability of less than 1% in transfer function and ± 1 degree in phase over the frequency range of interest. Finally, a calibration test was performed with the two microphones placed with their sensitive diaphragms facing each other at a separation distance of 1/32 inch. In this configuration both microphones are

exposed to the same acoustic field. Test results are shown in Figure 4.

The influence of instrumentation system characteristics on the estimated impedances may be determined from the test results obtained with the two microphones placed face to face. Denoting the calibration transfer function by $H_c(\omega)$, and the test measurement transfer function by $H_m(\omega)$, the true measured impedance is

$$Z_m = \frac{i\omega d [H_c(\omega) + H_m(\omega)]}{2 [H_c(\omega) - H_m(\omega)]} \quad (17)$$

Tests were made at two locations on the wall treatment near the forward end of the exhaust section of the ground run-up noise suppressor. The air temperature varied from approximately 70 degrees Fahrenheit for the first tests through 90 degrees Fahrenheit for the tests in the heat of the day. All test panels were in the shade while measurements were being performed. In calculations of impedance and absorption, an average value of 80 degrees Fahrenheit was used. Such an assumption leads to a maximum error of only 1% in the sound speed and 2% in air density.

3.4 Test Results

For each test, Microphone #2 was placed immediately next to the lining ($d_2 \approx 0.25$ in), and Microphone #1 at a predetermined distance from the wall. Tests were made for microphone spacings (d_{12}) of 0.75, 1.5, 3.0, 6.0, 12.0, 24.0, 36.0, and 48.0 inches. The individual microphone spectra, transfer function and coherency were plotted for each microphone spacing. Transfer function magnitude and phase values were also logged by hand for later entry into the absorption coefficient computer program. Sample test data are shown in Figure 5 for a microphone separation

distance of 1.5 inches.

A computer program was written using Equations (14)-(17), and values of absorption coefficient calculated for each test case. The resulting range of values is shown in Figure 6. Data scatter may be attributed to two different effects. First, the digital read-out of the measured data is rounded off to two decimal places for the transfer function magnitude, and to integer degrees for the phase. Such quantization can lead to errors when small differences between large vectors is concerned. Second, values of coherency less than 1.00 imply that there is contaminating noise in one or both signal channels. This is the case at larger microphone separations, particularly at frequencies where the reflected wave is in opposite phase to the incident wave, causing a pressure null. In these instances the calculated impedance and absorption values will be subject to random error.

In an effort to minimize the data scatter, two criteria based on acoustic wavelength were introduced. Data which did not satisfy either criterion were excluded from the analysis. Data were excluded at low frequencies if

$$\lambda > 60 d_{12}$$

and at high frequencies if

$$\lambda < 8 d_{12}.$$

Although somewhat arbitrary, these criteria were determined on the basis of the precision of the analyzer output and the interference between incident and reflected waves near to the test surface. In the case of the example shown in Figure 5 for a separation distance of 1.5 inches, data were assumed to be valid in the frequency range from 150 to 1140 Hz. Even with these restrictions, the data still exhibit the variability shown in Figure 6.

By averaging over the ensemble of absorption values obtained for various microphone spacing, it is possible to estimate a true value with reasonable confidence. This average value is also

shown in Figure 6 where it is compared with the theoretical value calculated (using the theory outlined in Section 2) on the basis of the lining configuration and material properties. Also, for convenience, the test results have been converted into average values for one-third octave frequency bands and again compared with corresponding predicted values. This comparison is presented in Figure 7.

The results in Figures 6 and 7 for normal incidence absorption coefficients show reasonably good agreement between measurements and predictions for the frequency range of interest below 500 Hz, although there is a significant discrepancy in the frequency range from 50 to 100 Hz. In general the results indicate that the normal incidence coefficient has a value of about 0.85 in the frequency range from 300 Hz to 500 Hz, and a value of about 0.8 in the frequency range from 150 Hz to 300 Hz. The measurements indicate that the value of 0.8 is achieved at frequencies down to about 60 Hz but the analysis shows a fall-off at frequencies below 120 Hz. It should be noted that the test procedure is itself experimental in that the importance of various parameters in determining the accuracy of the method is still to be determined. A detailed evaluation of the parametric effects was not possible within the scope of this project.

4.0 LINING ANALYSIS

4.1 Lining Materials and Configurations

In order to satisfy the immediate needs of NASA, the scope of the parametric study was restricted to a consideration of materials and dimensions already being considered for the wind tunnel lining or used in the B-1B ground run-up suppressor. This meant that the total thickness of the treatment had to lie in the range from 6 inches to 10 inches, and that the bulk material was either Owens-Corning PF 3350 or Type 703. However, Owens-Corning Type 701 was included in some cases, to represent a material with characteristics which lie between PF 3350 and 703.

It was assumed that the lining configuration consisted of an exterior perforated plate backed by a wire mesh screen and fiberglass cloth. This was followed by the bulk material, a second layer of fiberglass cloth (and, possibly, a second perforated plate), an air space and a rigid wall. Variations on this baseline configuration were evaluated, including removal of the air space; in that case the second layer of fiberglass cloth was also removed as it would serve no acoustic purpose.

Assumed properties of the materials are given in Table 1. The values are based on test data or are estimated but, in either case, they should be regarded as only nominal since there can be quite large variations from sample to sample, and test to test. Values of the properties are quoted for uncompressed PF 3350. However, only compressed PF 3350 was considered in the analysis since some compression is required in order to keep the material in place. An alternative fiberglass cloth was considered in some of the analyses. The cloth was assumed, arbitrarily, to have a flow resistance of 40.48 mks rays, i.e. one third that of the baseline cloth, a porosity of 0.5957, and a thickness of 0.007 in.

Table 1

Properties of Materials Assumed for Analysis

Owens-Corning PF 3350 (uncompressed):		
Density	(lb/cu.ft)	0.75
	(kg/cu.m)	12.0
Flow Resistivity	(mks rayls/m)	3400.0
Porosity		0.9952
Owens-Corning PF 3350 (9 ins compressed to 8 ins.):		
Density	(lb/cu.ft)	0.84
	(kg/cu.m)	13.5
Flow Resistivity	(mks rayls/m)	4100.0
Porosity		0.9946
Owens-Corning 701:		
Density	(lb/cu.ft)	1.6
	(kg/cu.m)	25.6
Flow Resistivity	(mks rayls/m)	14000.0
Porosity		0.9897
Owens-Corning 703:		
Density	(lb/cu.ft)	3.0
	(kg/cu.m)	48.0
Flow Resistivity	(mks rayls/m)	27000.0
Porosity		0.9808
Perforated Plate:		
22 Gauge, 33% open area		
Thickness	(inch)	0.0306
	(mm)	0.777
Hole Diameter	(inch)	0.09375
	(mm)	2.38
Wire Mesh Screen:		
Mesh 20 x20		
Diameter	(inch)	0.009
	(mm)	0.229
Porosity (Approx)		0.67
Fiberglass Cloth (Style 7628):		
Thickness	(inch)	0.007
	(mm)	0.178
Flow Resistance	(mks rayls)	121.42
Porosity		0.542
Structure Factor		6.2687

4.2 Parametric Study

The analytical model was used to investigate the effect of various design features and configurations for the proposed lining, as well as to explore the use of different materials. Several of the configurations evaluated were the result of queries from NASA personnel regarding possible inclusion or exclusion of certain items of the treatment. Other configurations followed from the design of the Rockwell B-1B noise suppressor. The results of the parametric study are given in this section.

The test results presented in Figures 6 and 7 are given in terms of the acoustic absorption coefficient for normally-incident (0°) sound waves. However, this does not represent a practical condition for the lining installation in the 80x120 wind tunnel. In the tunnel, there will be two situations of concern. First, sound waves propagating through the tunnel inlet will experience one or two reflections on the interior walls of the wind tunnel before passing through the inlet vanes. Thus it would be more appropriate to consider the absorption coefficient for an angle of about 45° instead of 0° . Secondly, the effect of the lining on the acoustic environment in the tunnel, for noise measurements in the test section, will depend more on the absorption coefficient averaged over all angles of incidence rather than one specific angle.

The influence of angle of incidence on the predicted acoustic absorption coefficient can be seen in Figure 8 which is associated with a 10-inch thickness of PF 3350 fiberglass material installed in a lining such as that identified as Configuration 1 in Figure 9. Figure 8 compares predicted absorption coefficient spectra for two angles of incidence, 0° and 45° , calculated using Equations (11) and (12), and the average or statistical absorption coefficient calculated using Equation (13). It is seen that the values of the coefficient associated with a 45° angle of incidence are similar

to the average values, and that in both cases the values are higher than those predicted for a 0° angle of incidence, throughout the frequency range of interest. Consequently, the results for the parametric study are given in terms of the absorption coefficient calculated for an angle of incidence of 45° .

Results from the parametric study are presented in Figures 10 through 17. The lining configurations considered in the figures are summarized in Figure 9, the main differences between the configurations being the presence or absence of an air space or a second perforated plate. The discussion regarding the figures can be best presented by means of brief comments on the effects of each of the parameters considered.

Blanket Material:

The lining originally considered for the 80x120 wind tunnel contained Owens Corning 703 (or similar) fiberglass for the sound absorbing blanket. However, the present analysis (Figure 10) indicates that an alternative material, such as Owens Corning PF 3350, which has a lower flow resistivity, would provide better sound absorption over a fairly wide frequency range below 2000 Hz when both materials have a thickness of 10 inches. The difference in absorption coefficient is less significant when the comparison is between Owens Corning 701 and PF 3350 (Figure 11), since 701 has a flow resistivity which lies between those of 703 and PF 3350. Only at very low frequencies (below 50 Hz in the case of 703 and 63 Hz for 701) is the material with the higher flow resistivity associated with the higher estimated absorption coefficient. In both comparisons the lining is assumed to be that of Configuration 1, since that was the configuration initially considered for the tunnel.

Lining Thickness:

The influence of the thickness of the lining is shown in Figures 10 through 12, where it is seen that the absorption coefficient at low frequencies becomes more dependent on thickness as the flow resistivity decreases. Thus an increase in material thickness from 6 inches to 10 inches has little effect on the absorption coefficient in the frequency range of interest when the material is Owens Corning 703 but has a significant effect when the material is PF 3350. At high frequencies the thickness of the treatment has no significant effect on the sound absorption coefficient.

Air Space:

The use of an air space or air gap between the porous material and the rigid wall can sometimes provide an improvement in low frequency absorption, although this might be at the expense of reduced acoustic performance at high frequencies. The reduction in the amount of material required might also result in a cost savings. However, the present analysis indicates that, for the PF 3350 material, the presence of the air gap (Configuration 2) has a negligible effect on the absorption coefficient (Figure 13), when the total thickness of the lining remains constant.

Fiberglass Cloth:

The influence of the flow resistance of the fiberglass cloth on predicted acoustic absorption characteristics of the lining is shown in Figure 14. The calculations were performed for a lining of the type shown by Configuration 1 in Figure 9. Three spectral curves are presented in Figure 14, one being associated with the baseline cloth (Style 7628) which has a nominal flow resistance of 121.4 mks rayls, and another with a configuration without fiberglass cloth. The third curve is associated with an

intermediate flow resistance of 40.48 mks rayls, which is about one third that of the baseline. It is seen that the absence of the cloth reduces the predicted absorption at frequencies below about 2000 Hz, but the predicted coefficients associated with the two cloth flow resistances are similar in value.

Perforated Backing Plate:

Configuration 3 in Figure 9 shows a lining in which a second perforated plate is introduced, this plate being placed between the inner layer of fiberglass cloth and the air gap. The configuration represents the lining shown in Figure 2, the second perforated plate being needed to provide structural rigidity and compression of the PF 3350 fiberglass. Analysis of Configuration 3 indicates that the second porous plate provides little benefit to the acoustic performance of the total lining (Figure 15). Thus the second plate has been excluded from most of the analyses.

Perforated Plate Thickness:

Most of the analyses of lining absorption coefficient were performed under the assumption that the perforated plate had a thickness of 0.0306 inch (22 gauge). However, experience suggests that the plate thickness should be greater for structural reasons. The effect of increased plate thickness on acoustic absorption coefficient will occur only at high frequencies, as can be seen in Figure 16 where predictions are compared for linings with perforated plates of 12 and 22 gauge. Consequently, changes of plate gauge within a realistic range of values should have only a small influence on the lining acoustic absorption coefficients.

Perforated Plate Open Area:

Figure 17 indicates that an increase in the open area of the perforated plate from 33% to 40% would cause a small decrease in

the lining absorption coefficient at low frequencies and a small increase at high frequencies.

4.3 Protection from Erosion

Since the lining will be exposed to the tunnel airflow, jet engine exhausts and turbulence from helicopter rotor wakes it will be necessary to prevent erosion of the fiberglass material. Furthermore, protection will be required to prevent damage by workers in the test section during model set-up and tear-down. The protection is provided by the perforated plate, wire mesh screen and fiberglass cloth shown in the three configurations depicted in Figure 9. Protection of this type is recommended by various sources including Beranek [4]. Figure 18, taken from Reference 4, shows recommended protective facings for sound absorbing linings exposed to gas flow of various speeds. In the case of the 80x120 wind tunnel test section it is understood that the tunnel flow speed can be as high as 160 ft/sec. Figure 18 shows that the recommended facing consists of a perforated plate, wire mesh screen and fiberglass cloth.

It has been stated by some NASA personnel that the acoustic lining in the test section of the Ames 40x80 wind tunnel does not contain a wire mesh screen and that no erosion has been observed, even though the flow velocities are higher than will be experienced in the 80x120 tunnel. However, in the absence of strong evidence regarding the condition of the lining and length of time that it has been exposed to high flow speeds, it is recommended that the wire mesh screen be included in the lining for the 80x120 tunnel. The recommended wire mesh screen is that given in Table 1; it has a large open area and has no influence on the acoustic performance of the lining.

5.0 CONCLUSIONS

As the result of the short parametric study, certain conclusions can be drawn regard design features of a sound absorbing lining for the Ames 80x120 wind tunnel. The model itself has been validated for normal-incidence sound, by means of an acoustic test on the wall panels of a Rockwell B-1B ground run-up noise suppressor.

The conclusions can be summarized as follows:

Sound absorption in the low to mid-frequency range can be increased by the use of PF 3350 fiberglass (nominal flow resistivity 4100 mks rayls) instead of Owens Corning 703 fiberglass (27,000 mks rayls) and by an increase in lining thickness from 6 inches to 10 inches.

When PF 3350 fiberglass is used, the acoustic absorption coefficients predicted for 10 inches of material are essentially the same as those for 8 inches of material plus a 2-inch air gap.

The presence of the fiberglass cloth improves the sound absorption of the lining, but there appears to be reasonable latitude in the choice of flow resistance of the cloth.

Increasing the thickness of the perforated plate from 22 gauge to 12 gauge, increasing the plate open area from 33% to 40%, or introducing a perforated backing plate has only a small effect on the predicted sound absorption coefficient. It is recommended that the perforated plate be thicker than 22 gauge, for structural reasons.

The installation of a wire mesh screen between the perforated face plate and the fiberglass cloth is recommend for erosion

protection. The mesh should be sufficiently open that it does not affect the acoustic performance of the lining. Representative characteristics of the wire mesh screen are given in Table 1.

REFERENCES

1. Anon, "Standard Test Method for Sound Absorption and Sound Absorption Coefficients by the Reverberation Room Method", ASTM Standard C 423-84a, (1984).
2. D.C. Rennison, J.F. Wilby, C.G. Gordon, "Design Concepts for Sound Absorbing Linings in the Test Section of the NASA Ames 80x120 Foot Wind Tunnel", NASA CR-152155, (1978).
3. C. Zwikker, C.W. Kosten, Sound Absorbing Materials, Elsevier Press, (1949).
4. L.L. Beranek (Editor), Noise and Vibration Control, McGraw-Hill Book Co., New York, (1971). See Chapter 10, "Acoustic Properties of Porous Materials", by D.A. Bies.
5. U. Ingard, R.H. Bolt, "Absorption Characteristics of Acoustic Material with Perforated Facings", J. Acoust. Soc. Amer., 23, 5, 533-540, (1951).
6. A.W. Guess, "Calculation of Perforated Plate Liner Parameters from Specified Acoustic Resistance and Reactance", J. Sound and Vib., 40, 1, 119-137, (1975).
7. P.M. Morse, K.U. Ingard, Theoretical Acoustics, McGraw-Hill Book Co., New York, (1968).
8. J.F. Allard, B. Sieben, "Measurements of Acoustic Impedance in a Free Field with Two Microphones and a Spectrum Analyzer", J. Acoust. Soc. Amer., 77, 4, 1617-1618, (1985).

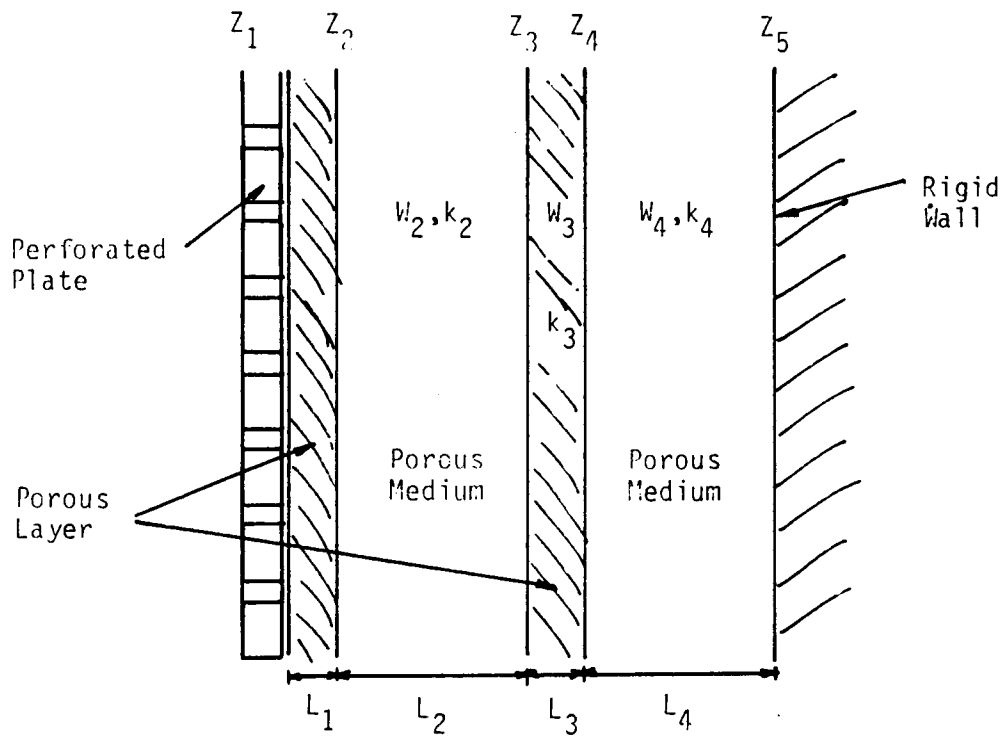


FIGURE 1. SECTION THROUGH MULTI-ELEMENT LINING

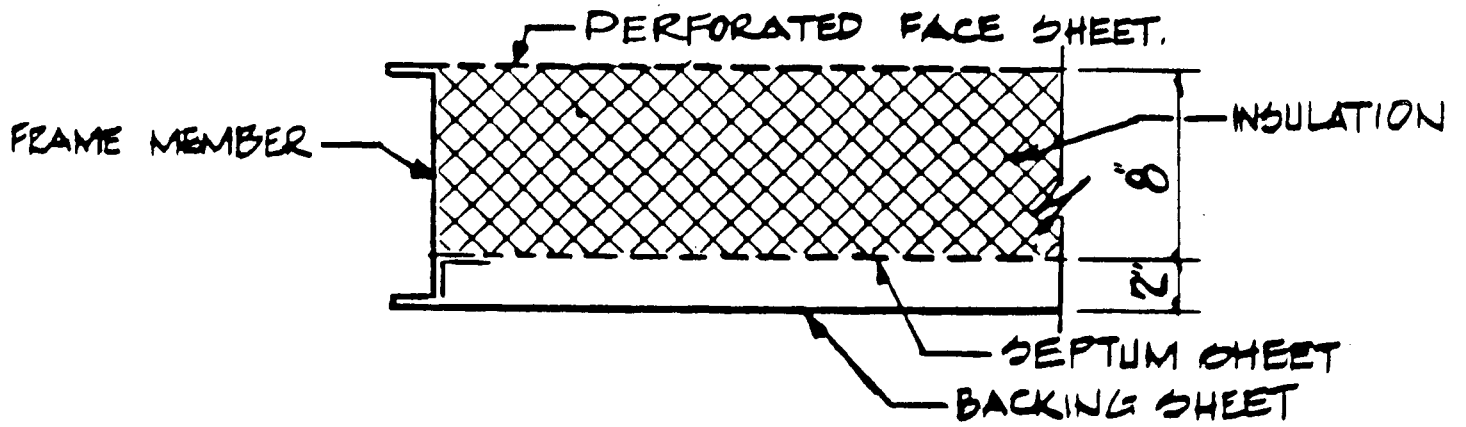


FIGURE 2. SECTION THROUGH TYPICAL WALL TREATMENT FOR B-1B GROUND RUN-UP NOISE SUPPRESSOR

ORIGINAL PAGE IS
OF POOR QUALITY

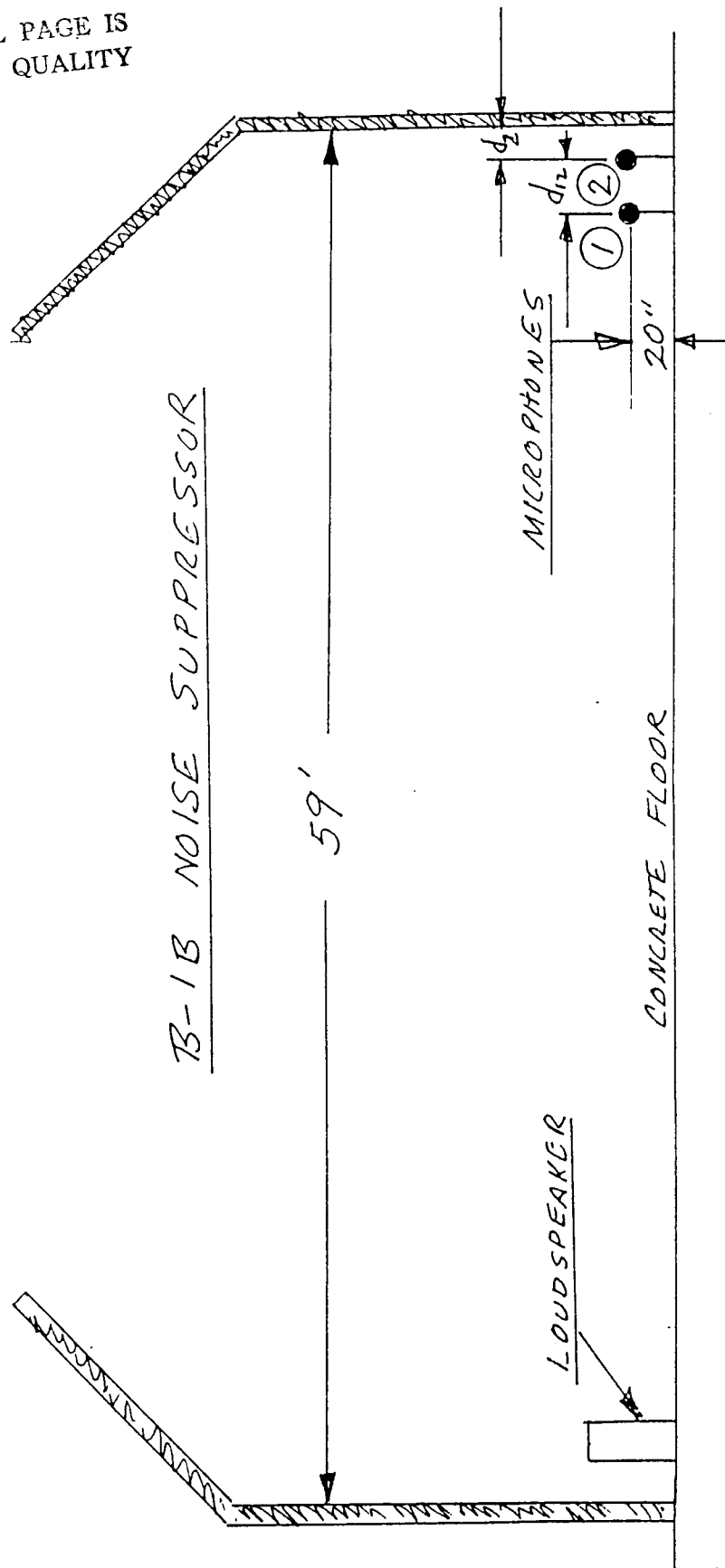
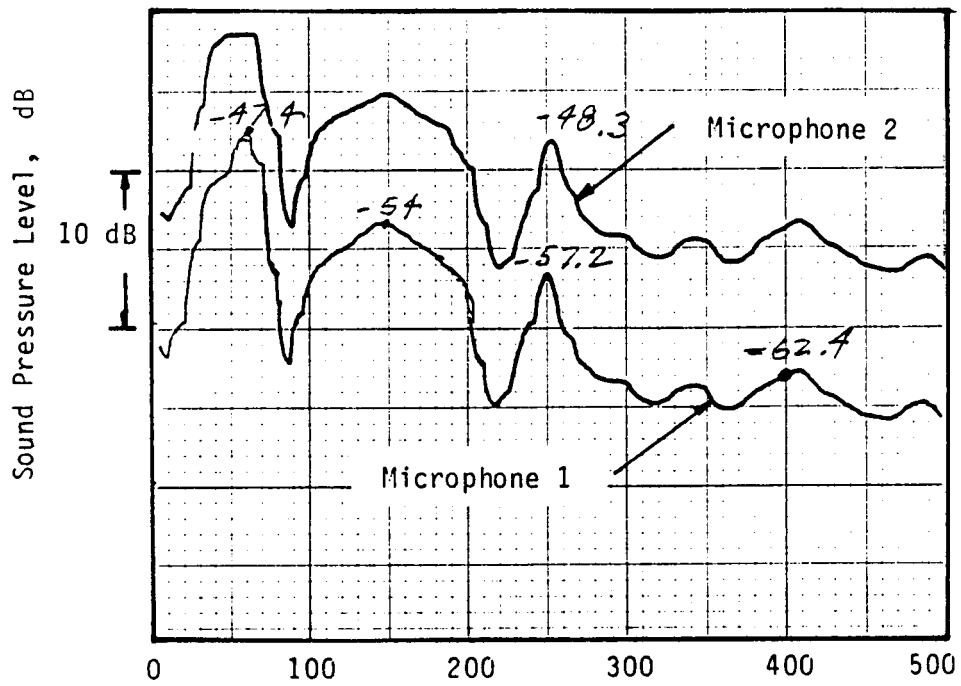


FIGURE 3. SKETCH OF TEST SET-UP

(a) Sound Pressure Levels at Microphone Locations



(b) Transfer Function Amplitude and Phase

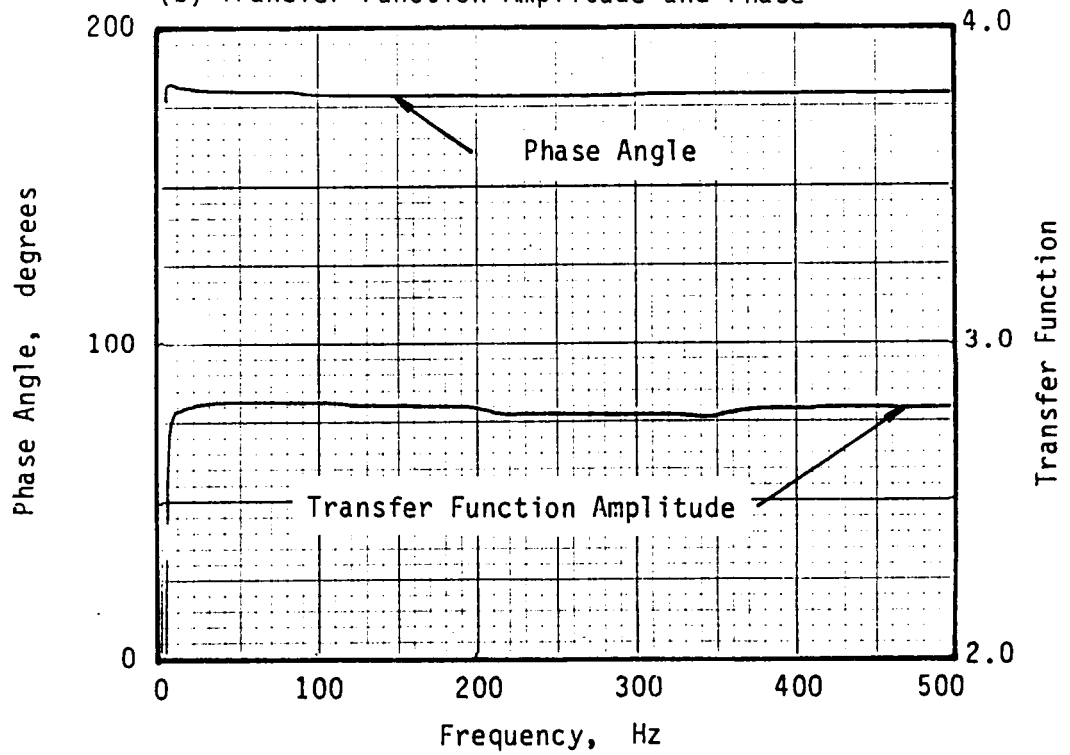
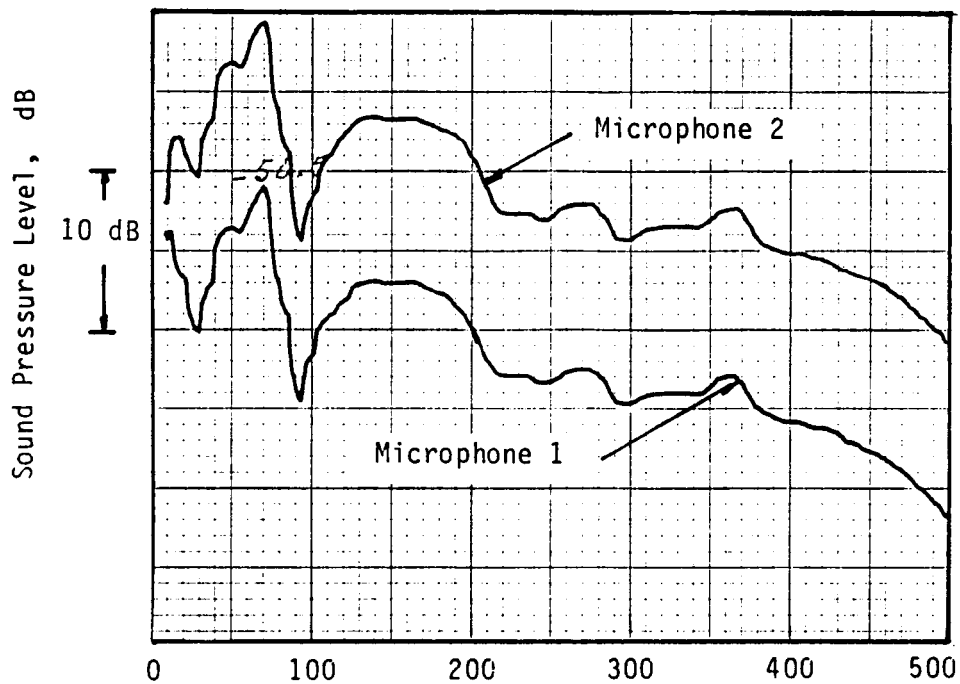


FIGURE 4. MICROPHONE CALIBRATION SPECTRA

(a) Sound Pressure Levels at Microphone Locations



(b) Transfer Function Amplitude and Phase

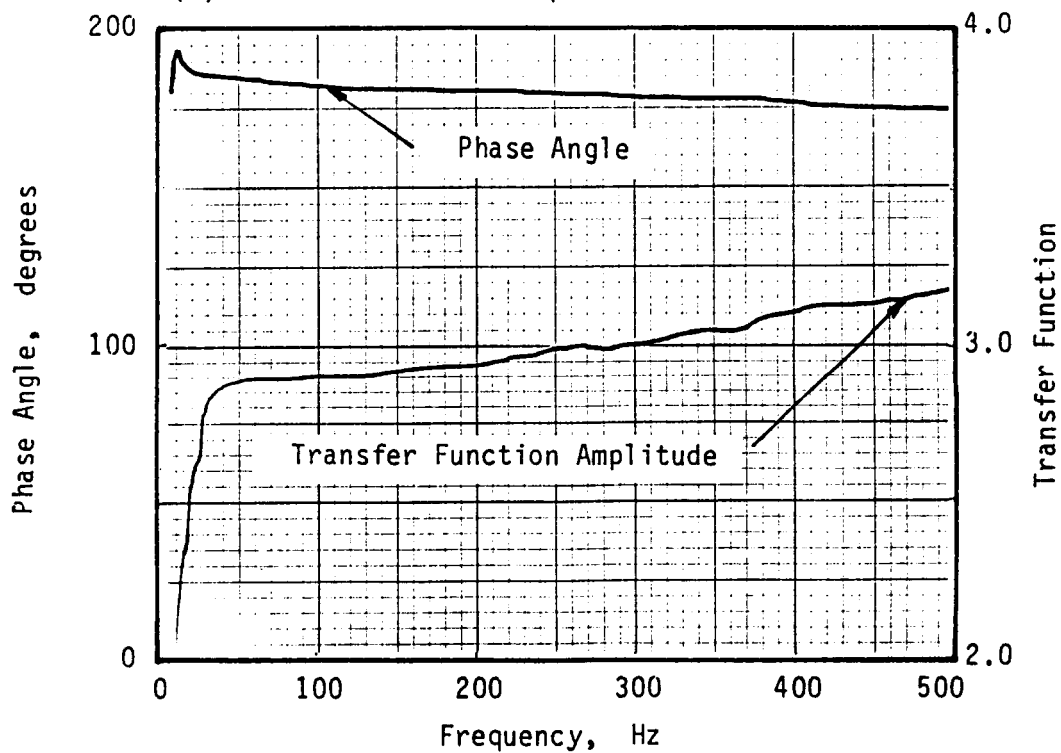


FIGURE 5. SAMPLE TEST DATA (MICROPHONE SEPARATION DISTANCE = 1.5 IN)

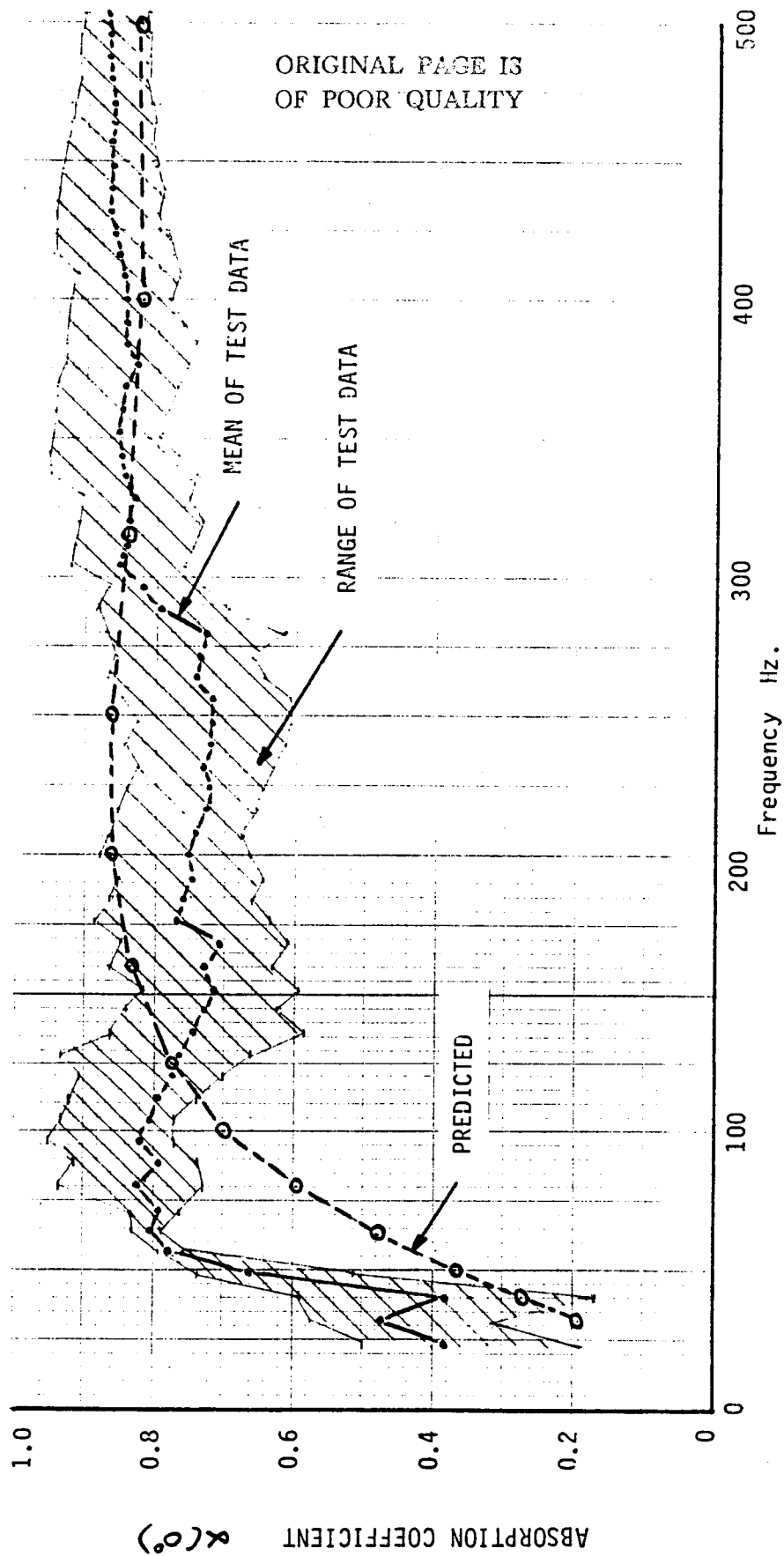


FIGURE 6. COMPARISON OF MEASURED AND PREDICTED SOUND ABSORPTION COEFFICIENTS FOR B-1B RUN-UP NOISE SUPPRESSOR

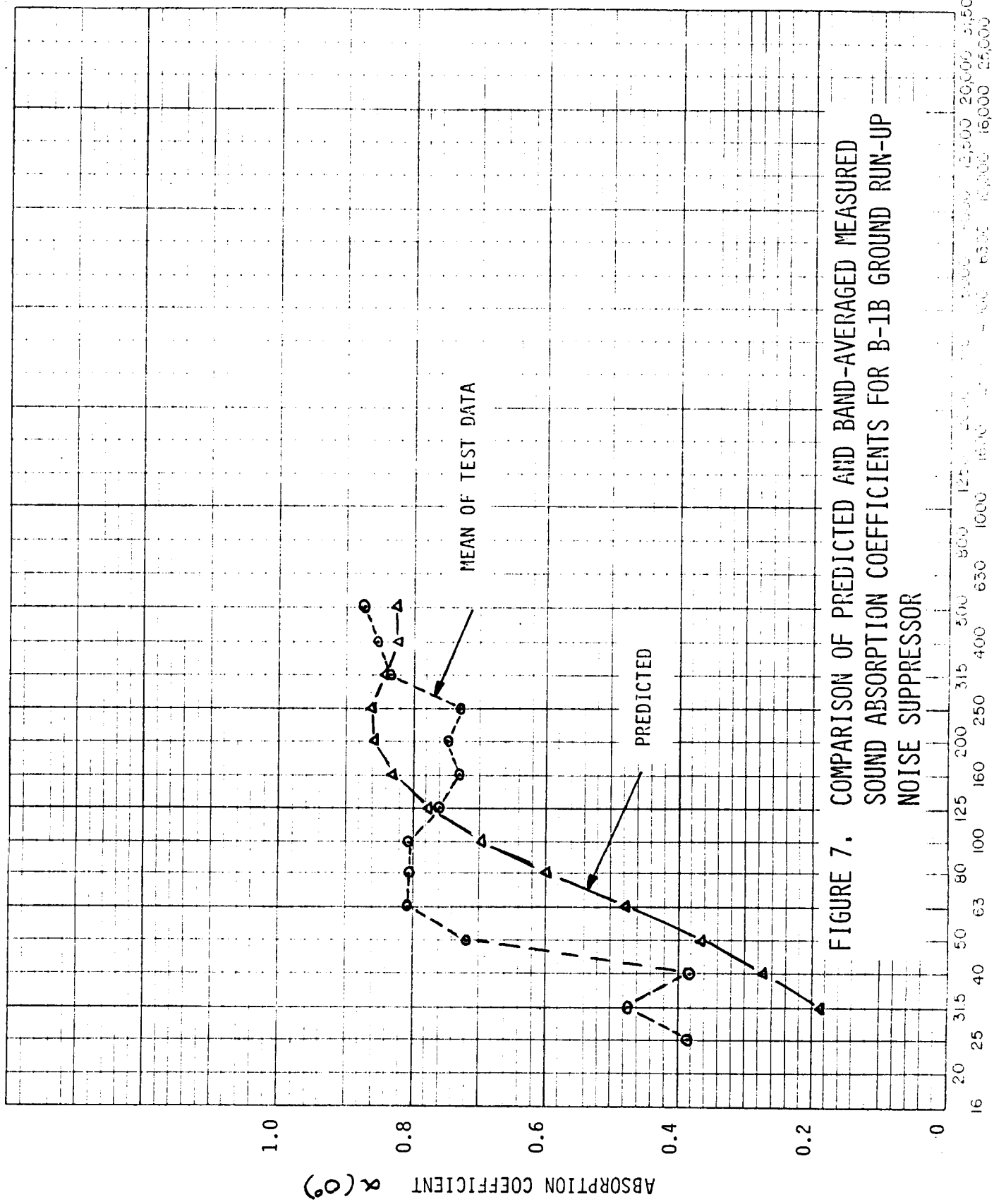


FIGURE 7. COMPARISON OF PREDICTED AND BAND-AVERAGED MEASURED SOUND ABSORPTION COEFFICIENTS FOR B-1B GROUND RUN-UP NOISE SUPPRESSOR

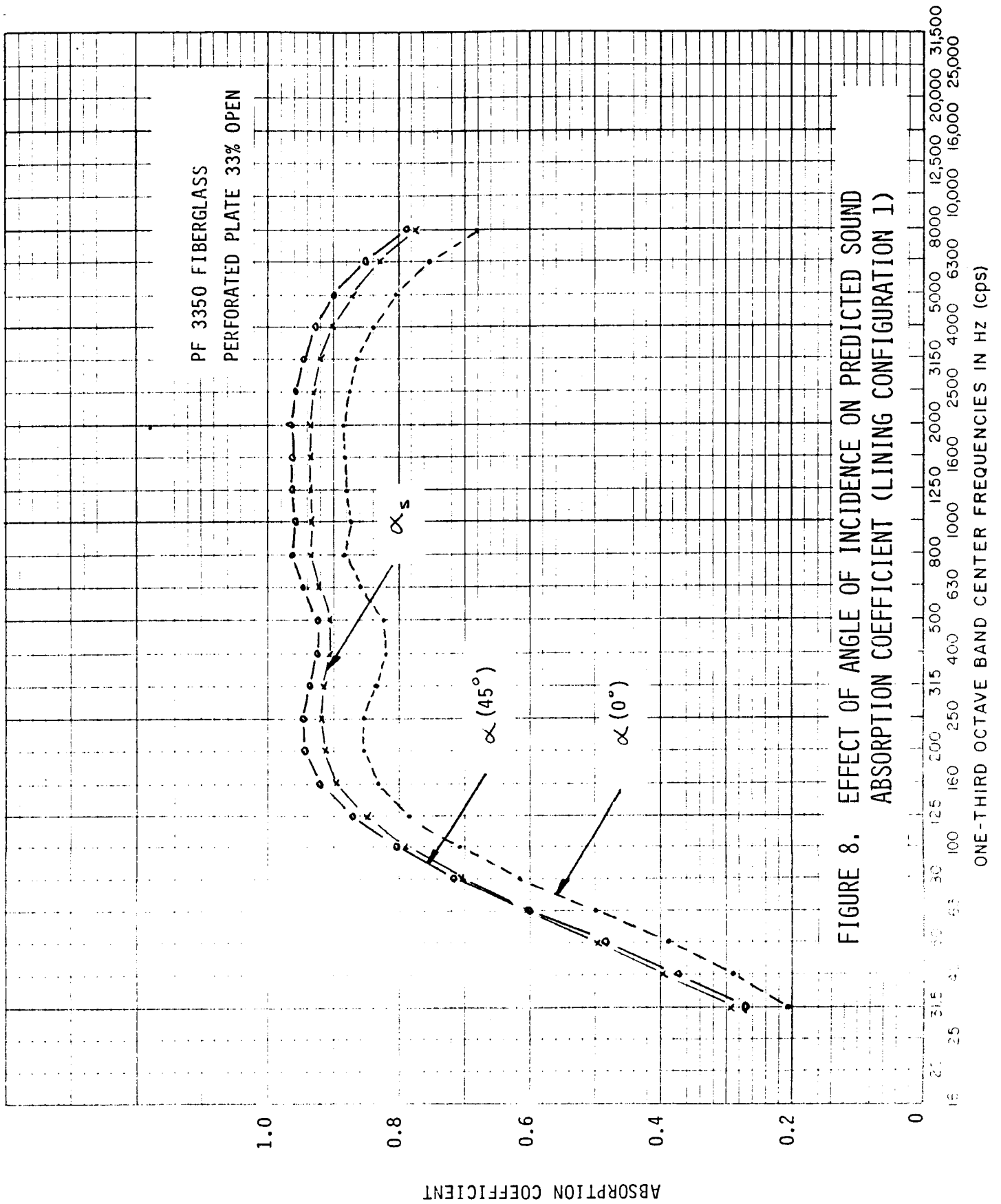
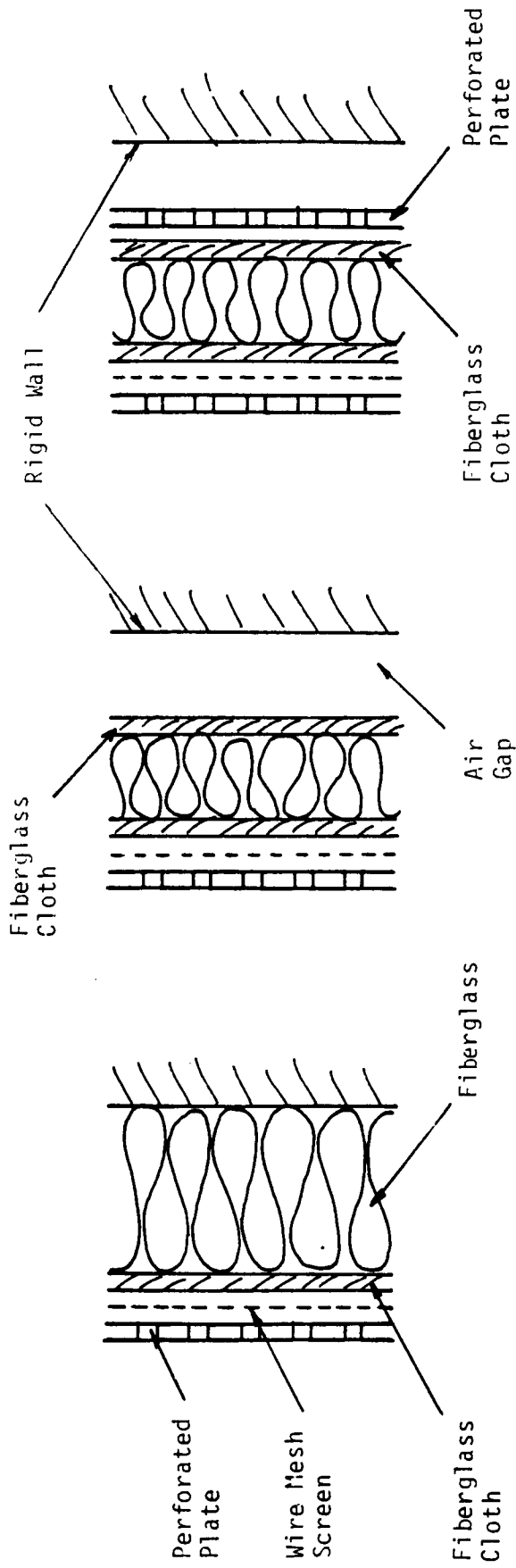


FIGURE 8. EFFECT OF ANGLE OF INCIDENCE ON PREDICTED SOUND ABSORPTION COEFFICIENT (LINING CONFIGURATION 1)



Configuration 1

Configuration 2

Configuration 3

FIGURE 9. LINING CONFIGURATIONS CONSIDERED IN ANALYSIS

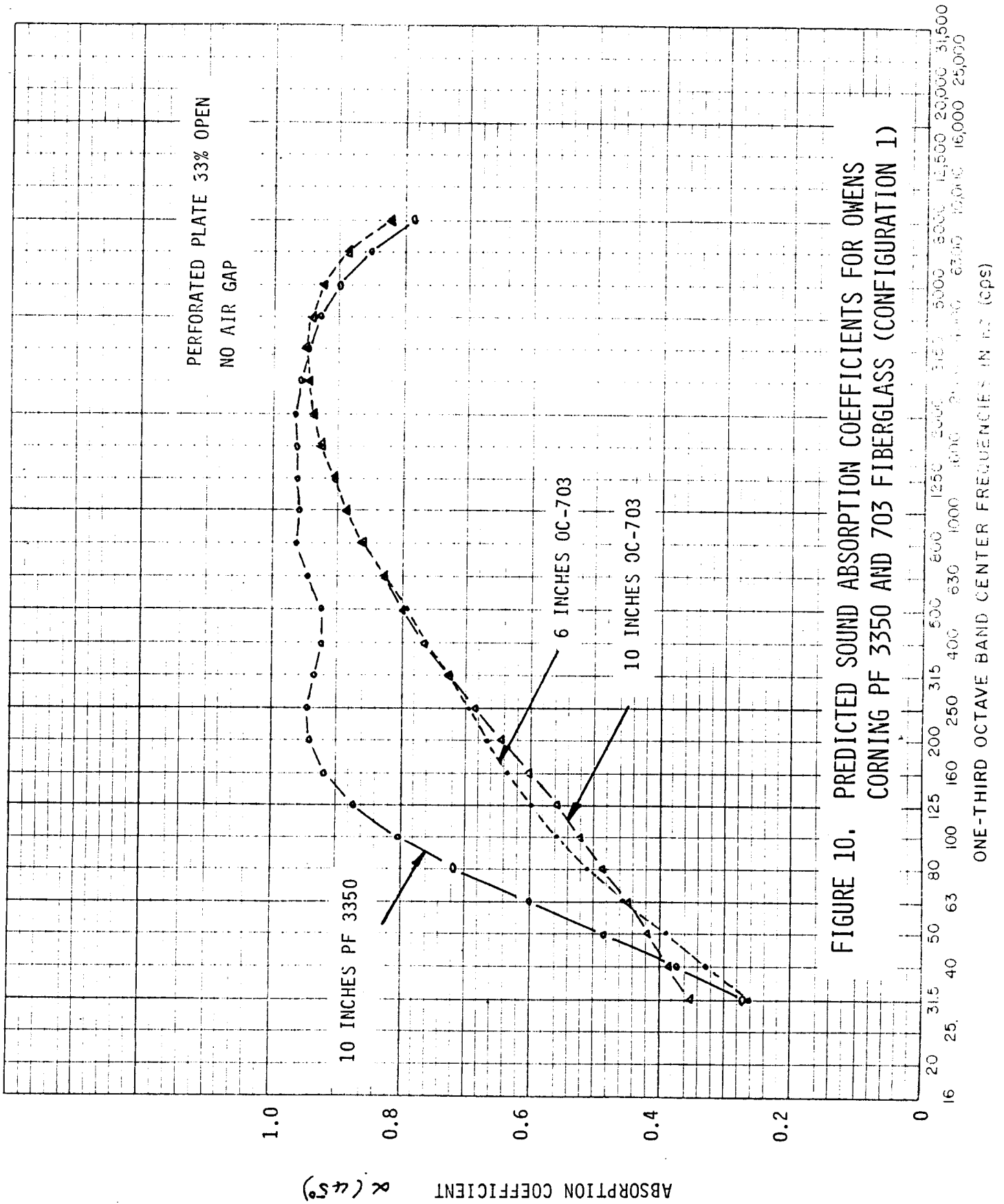
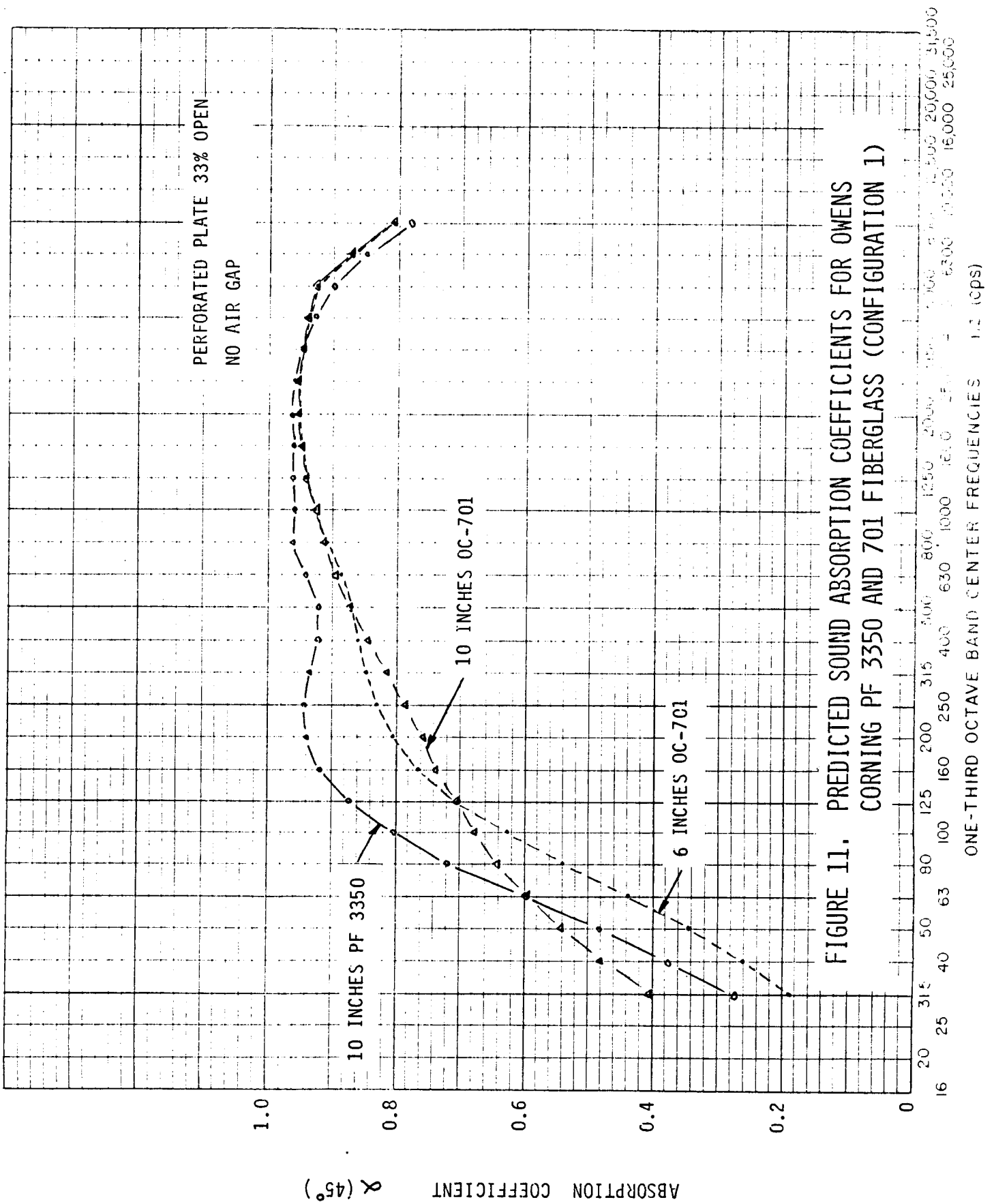


FIGURE 10. PREDICTED SOUND ABSORPTION COEFFICIENTS FOR OWENS CORNING PF 3350 AND 703 FIBERGLASS (CONFIGURATION 1)



ORIGINAL PAGE IS
OF POOR QUALITY

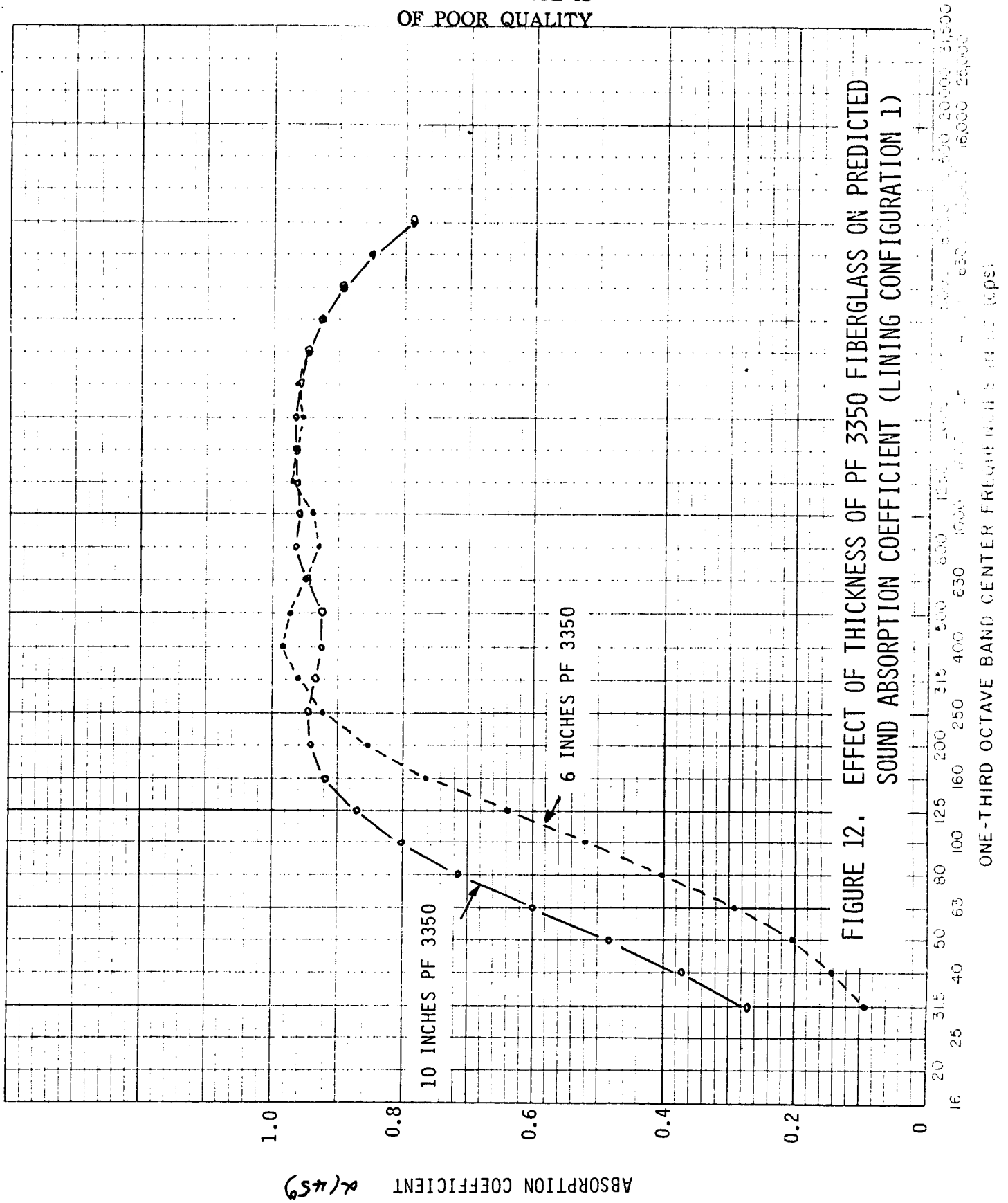


FIGURE 12. EFFECT OF THICKNESS OF PF 3350 FIBERGLASS ON PREDICTED SOUND ABSORPTION COEFFICIENT (LINING CONFIGURATION 1)

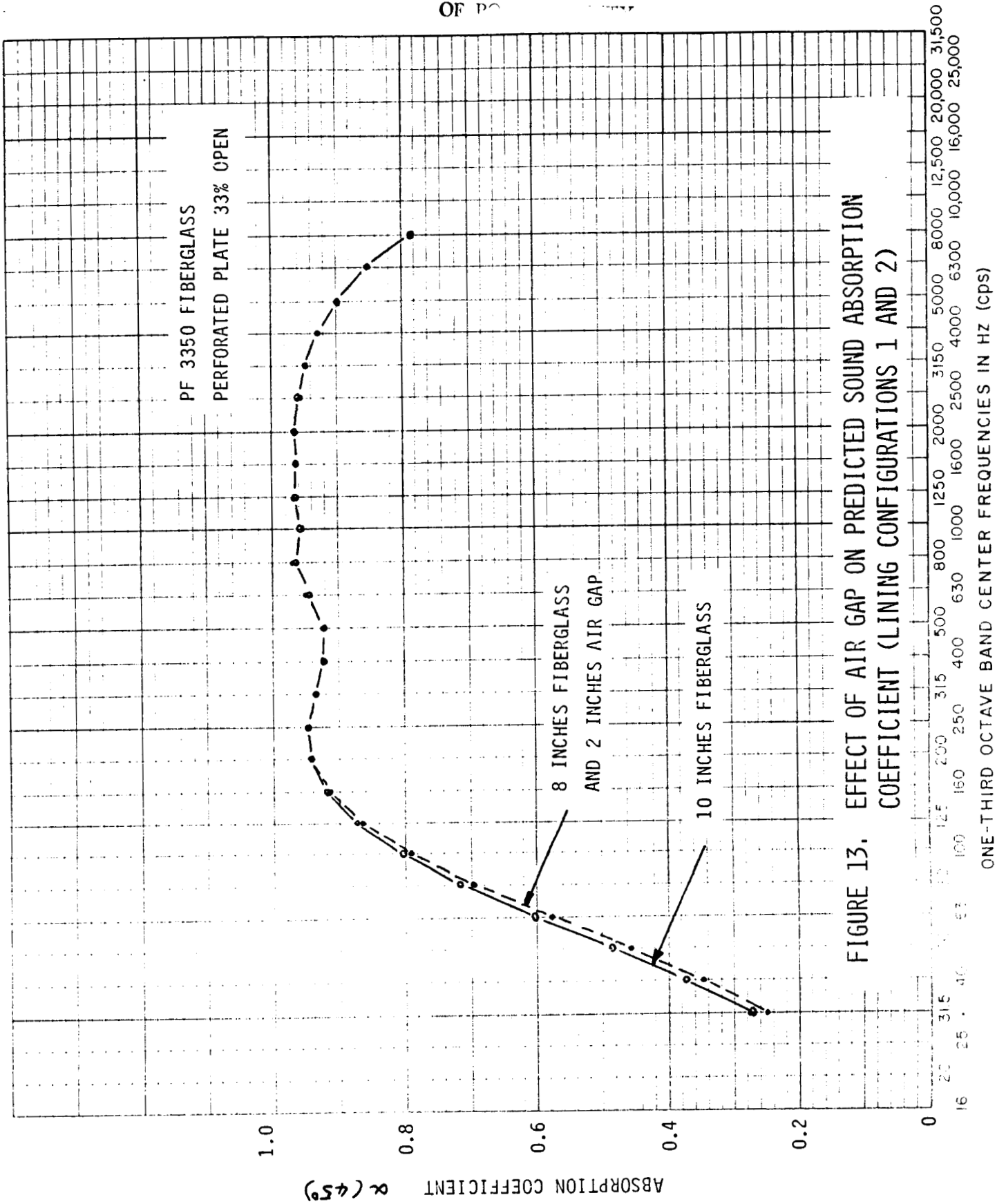


FIGURE 13. EFFECT OF AIR GAP ON PREDICTED SOUND ABSORPTION COEFFICIENT (LINING CONFIGURATIONS 1 AND 2)

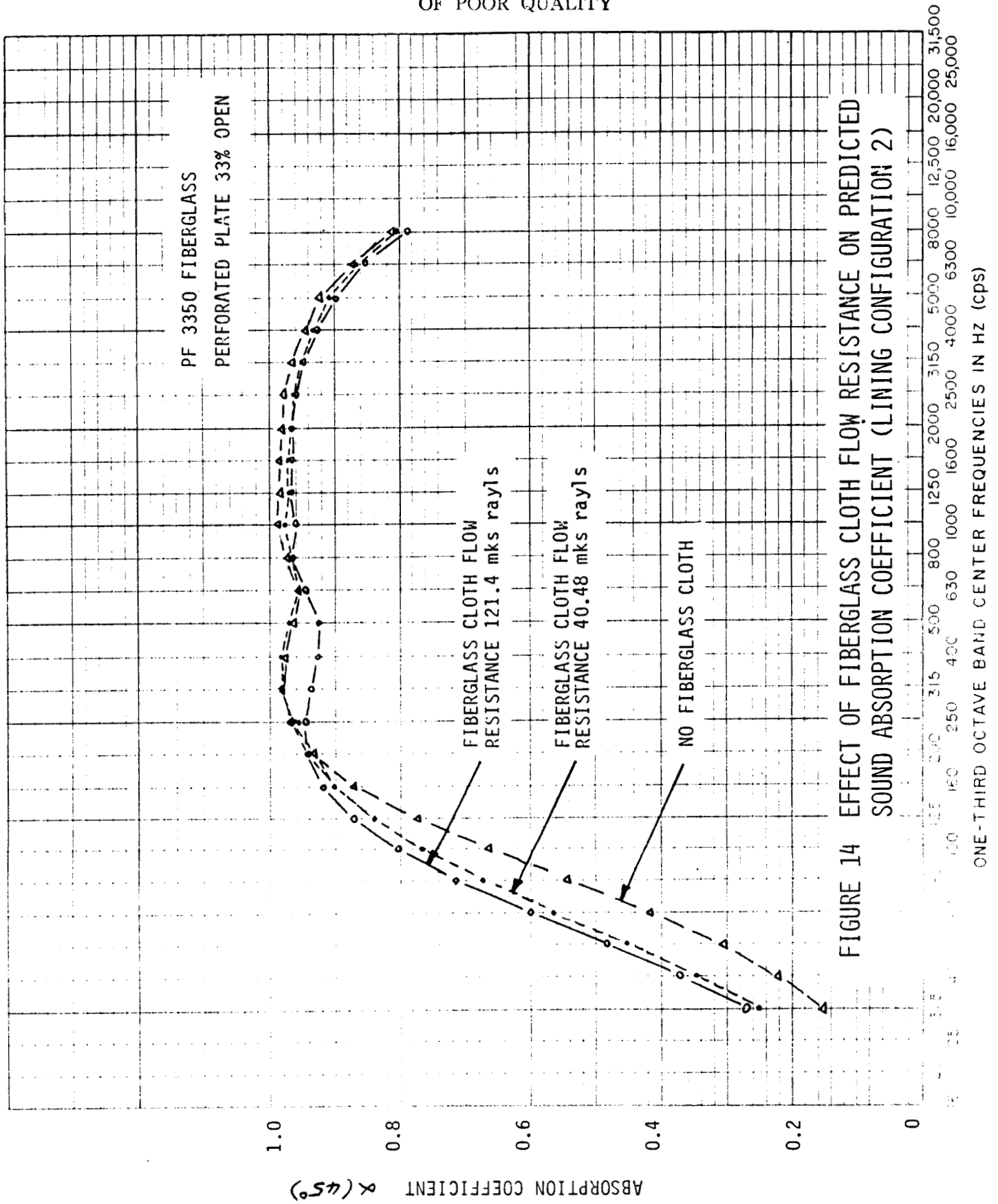


FIGURE 14 EFFECT OF FIBERGLASS CLOTH FLOW RESISTANCE ON PREDICTED SOUND ABSORPTION COEFFICIENT (LINING CONFIGURATION 2)

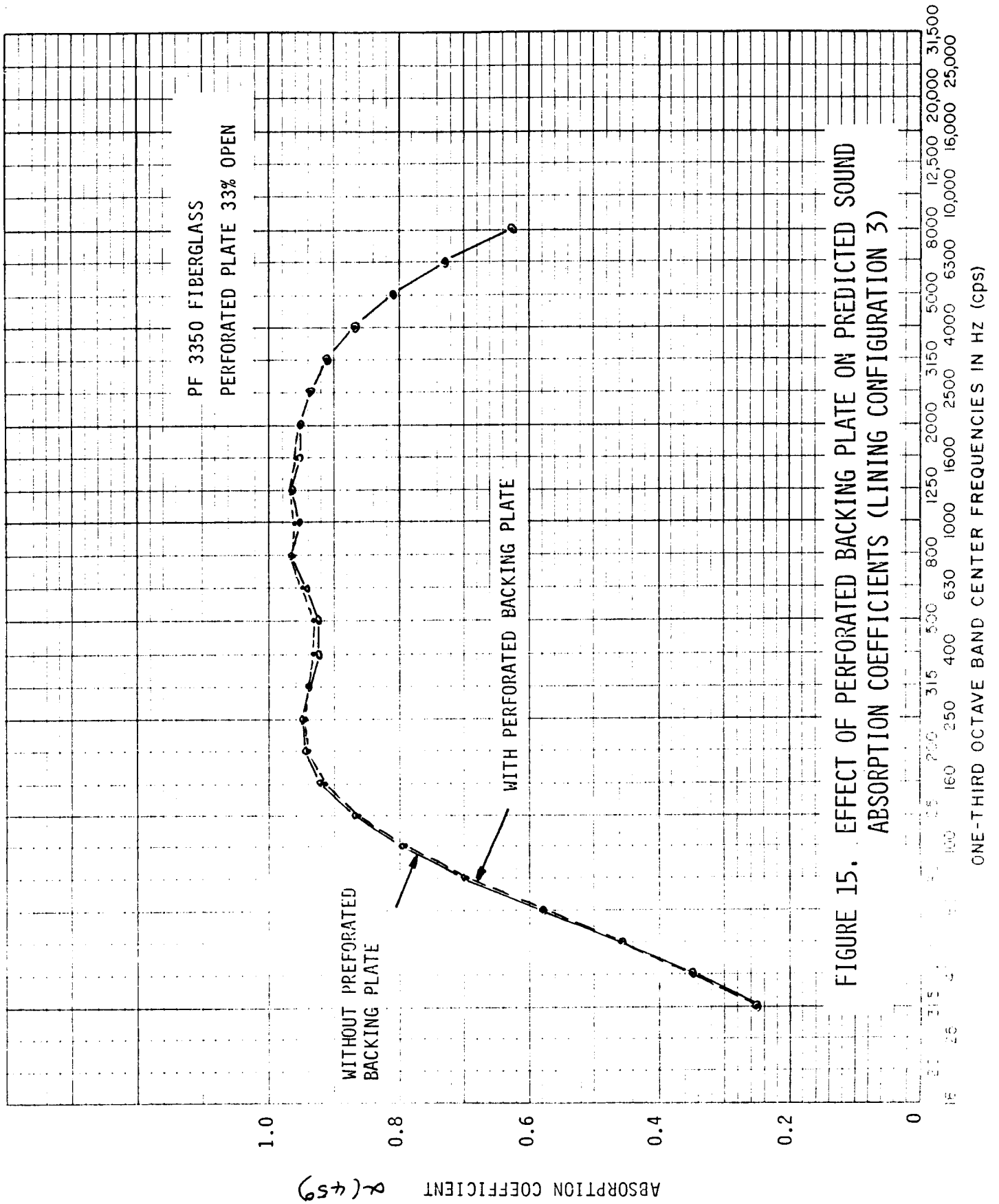


FIGURE 15. EFFECT OF PERFORATED BACKING PLATE ON PREDICTED SOUND ABSORPTION COEFFICIENTS (LINING CONFIGURATION 3)

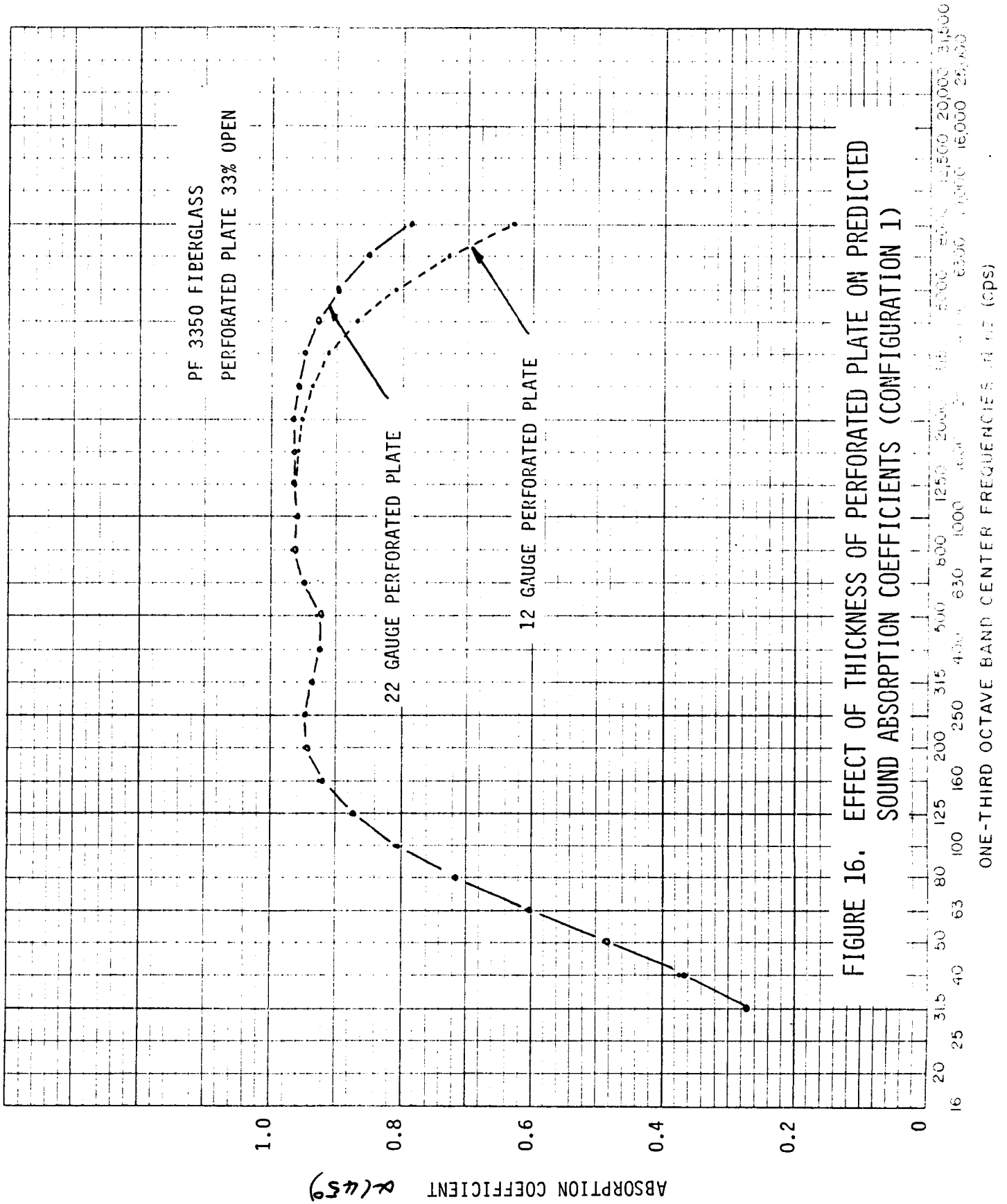


FIGURE 16. EFFECT OF THICKNESS OF PERFORATED PLATE ON PREDICTED SOUND ABSORPTION COEFFICIENTS (CONFIGURATION 1)

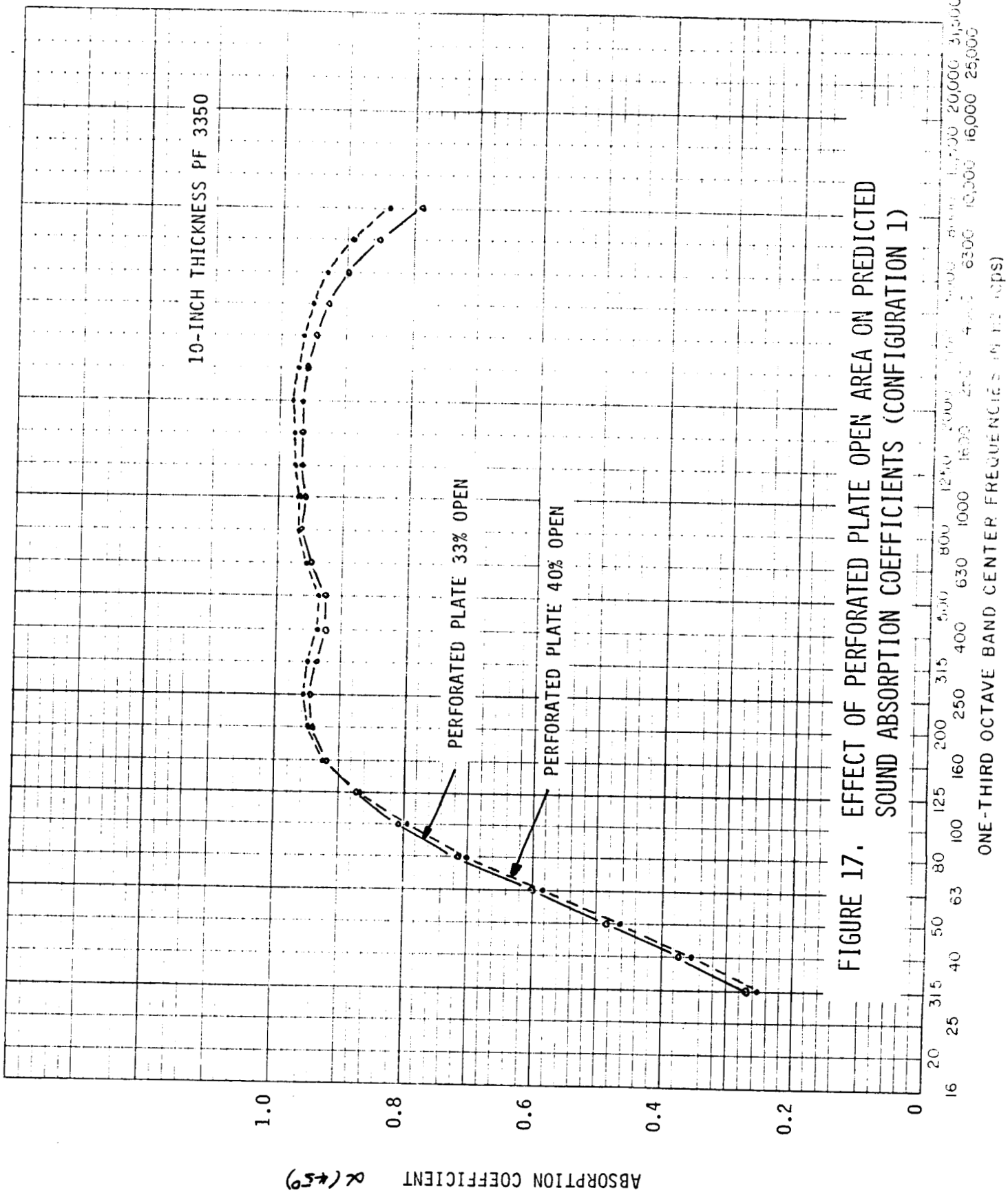
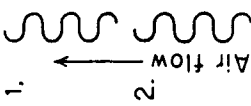
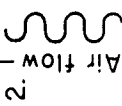
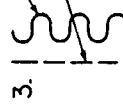
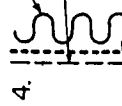
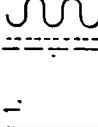
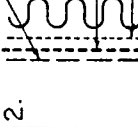
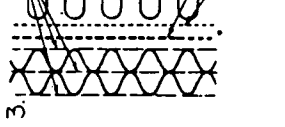


FIGURE 17. EFFECT OF PERFORATED PLATE OPEN AREA ON PREDICTED SOUND ABSORPTION COEFFICIENTS (CONFIGURATION 1)

Materials	Maximum allowable velocity in straight runs	Materials	Maximum allowable velocity in straight runs
<p>A. Ventilating ducts</p> <p>1. Uncoated lining, see Note 1</p>  <p>2. Coated lining, see Note 2</p>  <p>3. Blanket</p>  <p>4. Perforated facing as in 43</p>  <p>Glass fiber cloth</p>	<p>25 ft/sec 8 m/sec</p> <p>30 ft/sec 10 m/sec</p> <p>75 ft/sec 25 m/sec</p> <p>125 ft/sec 40 m/sec</p>	<p>B. Large panels (e.g., test cell applications)</p> <p>1. Same construction as A4</p>  <p>2. 20 gauge perforated metal, minimum 25% open area, Wire screen, Glass fiber cloth</p>  <p>3. Three layers 20 gauge perforated metal, minimum 25% open area, shown separated by 2 corrugated perforated sheets, Wire screen, Glass fiber cloth, Blanket</p> 	<p>75 ft/sec 25 m/sec</p> <p>180 ft/sec 60 m/sec</p> <p>300 ft/sec 100 m/sec</p>

- Notes: 1. Examples of suitable materials: Johns-Manville, Microtex, Micro-bar, Micro-Coustic.
 2. Examples of suitable materials: Johns-Manville, Microlite, Tenu-Mat, Microtex; Gustin Bacon, Ultra * Liner; Owens-Corning, Fiberglas.

FIGURE 18. PROTECTIVE FACINGS FOR ACOUSTICAL LININGS SUBJECTED TO HIGH VELOCITY GAS FLOWS (REFERENCE 4)

1. Report No. NASA CR-177396	2. Government Accession No.	3. Recipient's Catalog No.	
4. Title and Subtitle AN ANALYSIS OF SOUND ABSORBING LININGS FOR THE INTERIOR OF THE NASA AMES 80X120-FOOT WIND TUNNEL.		5. Report Date November 1985	
		6. Performing Organization Code	
7. Author(s) J.F. Wilby, P.H. White		8. Performing Organization Report No. 7066-01	
		10. Work Unit No.	
9. Performing Organization Name and Address Astron Research and Engineering 3228 Nebraska Avenue Santa Monica, CA 90404		11. Contract or Grant No. A-32501-C	
		13. Type of Report and Period Contractor Report	
12. Sponsoring Agency Name and Address National Aeronautics and Space Administration Washington, DC 20546		14. Sponsoring Agency Code 505-43-01	
		15. Supplementary Notes Paul T. Soderman NASA Ames Technical Monitor: Ames Research Center, MS:247-1 (415)694-6678/FTS:464-6678 Moffet Field, CA 94035	
16. Abstract It is desirable to achieve low frequency sound absorption in the test section of the NASA Ames 80X120 ft. wind tunnel. However, it is difficult to obtain information regarding sound absorption characteristics of potential treatments because of the restrictions placed on the dimensions of the test chambers. In the present case measurements were made in a large enclosure for aircraft ground run-up tests. The normal impedance of the acoustic treatment was measured using two microphones located close to the surface of the treatment. The data showed reasonably good agreement with analytical methods which were then used to design treatments for the wind tunnel test section. A sound-absorbing lining is proposed for the 80X120-ft. wind tunnel.			
17. Key Words (Suggested by Author(s)) Sound absorption Low frequency Acoustic impedance Wind tunnel lining		18. Distribution Statement Unclassified-Unlimited Subject Category 71	
19. Security Classif. (of this report) Unclassified	20. Security Classif. (of this page) Unclassified	21. No. of Pages 44	22. Price*